



OPEN ACCESS

EDITED BY

Julio Plaza-Diaz,
Children's Hospital of Eastern Ontario
(CHEO), Canada

REVIEWED BY

Laura Mitrea,
University of Agricultural Sciences and
Veterinary Medicine of Cluj-Napoca, Romania
Telek Bernadette-Emoke,
University of Agricultural Sciences and
Veterinary Medicine of Cluj-Napoca, Romania

*CORRESPONDENCE

Yunlong Hou
✉ houyunlonghrb@hotmail.com
Yiling Wu
✉ professorsylw@163.com

[†]These authors have contributed equally to
this work and share first authorship

RECEIVED 12 October 2023

ACCEPTED 18 December 2023

PUBLISHED 08 January 2024

CITATION

Zhang S, Li M, Chang L, Mao X, Jiang Y,
Shen X, Niu K, Lu X, Zhang R, Song Y, Ma K,
Li H, Wei C, Hou Y and Wu Y (2024) Bazi
Bushen capsule improves the deterioration of
the intestinal barrier function by inhibiting
NLRP3 inflammasome-mediated pyroptosis
through microbiota-gut-brain axis.
Front. Microbiol. 14:1320202.
doi: 10.3389/fmicb.2023.1320202

COPYRIGHT

© 2024 Zhang, Li, Chang, Mao, Jiang, Shen,
Niu, Lu, Zhang, Song, Ma, Li, Wei, Hou and
Wu. This is an open-access article distributed
under the terms of the [Creative Commons
Attribution License \(CC BY\)](https://creativecommons.org/licenses/by/4.0/). The use,
distribution or reproduction in other forums is
permitted, provided the original author(s) and
the copyright owner(s) are credited and that
the original publication in this journal is cited,
in accordance with accepted academic
practice. No use, distribution or reproduction
is permitted which does not comply with
these terms.

Bazi Bushen capsule improves the deterioration of the intestinal barrier function by inhibiting NLRP3 inflammasome-mediated pyroptosis through microbiota-gut-brain axis

Shixiong Zhang^{1,2†}, Mengnan Li^{2,3†}, Liping Chang^{2,3},
Xinjing Mao^{1,2}, Yuning Jiang^{1,2}, Xiaogang Shen^{3,4}, Kunxu Niu^{3,4},
Xuan Lu^{2,4}, Runtao Zhang^{2,4}, Yahui Song^{3,4}, Kun Ma^{3,4},
Hongrong Li^{2,3}, Cong Wei^{2,3}, Yunlong Hou^{2*} and Yiling Wu^{1,2*}

¹College of Traditional Chinese Medicine, College of Integrated Traditional Chinese and Western Medicine, Nanjing University of Chinese Medicine, Nanjing, China, ²National Key Laboratory for Innovation and Transformation of Luobing Theory, Shijiazhuang, China, ³Key Laboratory of State Administration of TCM (Cardio-Cerebral Vessel Collateral Disease), Shijiazhuang, China, ⁴High-level TCM Key Disciplines of National Administration of Traditional Chinese Medicine—Luobing Theory, Shijiazhuang, China

Purpose: The senescence-accelerated prone mouse 8 (SAMP8) is a widely used model for accelerating aging, especially in central aging. Mounting evidence indicates that the microbiota-gut-brain axis may be involved in the pathogenesis and progression of central aging-related diseases. This study aims to investigate whether Bazi Bushen capsule (BZBS) attenuates the deterioration of the intestinal function in the central aging animal model.

Methods: In our study, the SAMP8 mice were randomly divided into the model group, the BZ-low group (0.5 g/kg/d BZBS), the BZ-high group (1 g/kg/d BZBS) and the RAPA group (2 mg/kg/d rapamycin). Age-matched SAMR1 mice were used as the control group. Next, cognitive function was detected through Nissl staining and two-photon microscopy. The gut microbiota composition of fecal samples was analyzed by 16S rRNA gene sequencing. The ileum tissue morphology was observed by hematoxylin and eosin staining, and the intestinal barrier function was observed by immunofluorescence. The expression of senescence-associated secretory phenotype (SASP) factors, including P53, TNF- α , NF- κ B, IL-4, IL-6, and IL-10 was measured by real-time quantitative PCR. Macrophage infiltration and the proliferation and differentiation of intestinal cells were assessed by immunohistochemistry. We also detected the inflammasome and pyroptosis levels in ileum tissue by western blotting.

Results: BZBS improved the cognitive function and neuronal density of SAMP8 mice. BZBS also restored the intestinal villus structure and barrier function, which were damaged in SAMP8 mice. BZBS reduced the expression of SASP factors and the infiltration of macrophages in the ileum tissues, indicating a lower level of inflammation. BZBS enhanced the proliferation and differentiation of intestinal cells, which are essential for maintaining intestinal homeostasis. BZBS modulated the gut microbiota composition, by which BZBS inhibited the activation of inflammasomes and pyroptosis in the intestine.

Conclusion: BZBS could restore the dysbiosis of the gut microbiota and prevent the deterioration of intestinal barrier function by inhibiting NLRP3 inflammasome-mediated pyroptosis. These results suggested that BZBS attenuated the cognitive aging of SAMP8 mice, at least partially, by targeting the microbiota-gut-brain axis.

KEYWORDS

intestinal barrier function, microbiota-gut-brain axis, inflammasome, pyroptosis, SAMP8

1 Introduction

Aging is the cause of many age-related diseases, which can lead to gradual decline in body function and increase the risk of age-related diseases (Gavrilov and Gavrilova, 2017). One of the key components of the body that is affected by aging is the intestinal barrier, which consists of the intestinal epithelium that protects the body from the external environment and adapts to various stimuli, including aging (El Maï et al., 2023; Salazar et al., 2023). Many studies have shown that aging has a significant impact on the structure and function of the intestine (Branca et al., 2019). It has been suggested that impaired intestinal barrier function is a major sign of aging (Suzuki et al., 2022; El Maï et al., 2023). Furthermore, intestinal barrier dysfunction and the resulting pathological damage are believed to be important mechanisms underlying aging (Funk et al., 2020; Salazar et al., 2023). Therefore, maintaining the integrity of the intestinal barrier could be an effective way to delay aging.

The senescence-accelerated prone mouse 8 (SAMP8) is a widely used model for aging research (Roig-Soriano et al., 2022), especially for brain cognition (Cristófol et al., 2012). Interestingly, some studies have found that the intestine of SAMP8 mice shows signs of aging before the brain does (Ben Othman et al., 2020; D'Antongiovanni et al., 2021). However, the exact changes that occur in the intestine of SAMP8 mice are still unclear. To explore this issue, we conducted a study on the intestinal aging process in SAMP8 mice. Previous studies have suggested that the aging of the gastrointestinal tract involves the degeneration of villi and the reduction of tight junction proteins, which are essential for maintaining the intestinal barrier (Soenen et al., 2016). However, the causes of intestinal barrier dysfunction due to aging are still unknown (Ma et al., 2020). Gut dysbiosis, or the imbalance of gut bacteria, can impair the intestinal barrier and trigger systemic inflammation, as shown by increased damage to the colon and liver and elevated levels of inflammatory markers (Haran and McCormick, 2021; Zhao et al., 2023). Moreover, endotoxins produced by gut bacteria, such as lipopolysaccharides (LPS), can also leak into the bloodstream (Li T. et al., 2023), which may activate the inflammasomes mediated by the NOD-like receptor family pyrin domain-containing 3 (NLRP3) pathway (Li Y. et al., 2023). Inflammasomes are protein complexes that regulate inflammation and cell death. Previous studies have shown that inhibiting the NLRP3 inflammasome can extend lifespan (Marín-Aguilar et al., 2020). Inflammasome activation can also induce pyroptosis, which is a type of cell death that involves inflammation

and tissue damage (Zheng and Kanneganti, 2020; Barnett et al., 2023). Therefore, we hypothesize that NLRP3 inflammasome activation and pyroptosis may play roles in intestinal barrier damage caused by aging. We aim to test this hypothesis in SAMP8 mice.

Bazi Bushen (BZBS) is a traditional Chinese medicine (TCM) that contains 16 herbs (*Semen Cuscutae*, *Fructus Lycii*, *Epimedii Folium*, *Fructus Schisandrae Sphenantherae*, *Fructus Cnidii*, *Fructus Rosae Laevigatae*, *Semen Allii Tuberosi*, *Radix Morindae Officinalis*, *Herba Cistanches*, *Fructus Rubi*, *Radix Rehmanniae Recens*, *Radix Cyathulae*, *Radix Ginseng*, *Cervi Cornu Pantotrichum*, *Hippocampus*, and *Fuctus Toosendan*), including the seeds of eight plants and other herbs such as *ginseng* and *Cistanche*. BZBS contains a variety of bioactive compounds with potential anti-aging properties. These compounds include ginsenosides, polyphenols, and crude polysaccharides (Hao et al., 2022), which have been shown to regulate oxidative stress, apoptosis, inflammation, and the microbe-gut-brain axis. Additionally, *Cistanche deserticola* polysaccharides, one of the key anti-aging compounds in BZBS, have been shown to alleviate cognitive decline in aging model mice by restoring the gut microbiota-brain axis (Gao et al., 2021). Furthermore, *Fructus Lycii*, another important constituent of BZBS, has been demonstrated to alleviate age-related bone loss by targeting BMPRIA/BMPRII/Noggin (Sun et al., 2023). These findings suggest that BZBS has the potential to delay the aging process by targeting multiple pathways that contribute to age-related decline. It is based on the ancient theory of kidney-tonifying, which is believed to enhance vitality and longevity. BZBS has been shown to mitigate epigenetic aging and extend health span in naturally aging mice (Mao et al., 2023). Furthermore, BZBS has demonstrated beneficial effects on aging-related diseases in various organs, especially in improving cognitive function (Ji et al., 2022; Wang et al., 2023). However, the potential of BZBS to delay aging by repairing intestinal damage caused by accelerated aging has not been explored yet.

Here, we studied how BZBS affects the aging and damage of the intestines in SAMP8 mice, which are a model of accelerated aging. We discovered that SAMP8 mice had cognitive problems and severe intestinal damage as they got older, and they lost their normal intestinal barrier function. BZBS improved their overall health and cognition and restored their intestinal barrier function. BZBS also reduced inflammation and senescence, increased intestinal cell growth and differentiation, changed the gut microbiota composition, and prevented pyroptosis, a type of cell death caused by inflammasomes. Our results suggest that BZBS could slow down aging by reversing the aging and damage of the intestines.

2 Materials and methods

2.1 Animal models and drugs

The 8-week-old male SAMP8 mice were provided by Peking University Health Science Center, and senescence-accelerated mouse resistant 1 (SAMR1) mice were selected as the control group. The mice were kept at constant environmental conditions of $22 \pm 2^\circ\text{C}$, $55 \pm 10\%$ relative humidity and a 12 h/12 h light/dark cycle. All mice were adaptively fed for 1 week. Then, the SAMP8 mice were randomly divided into four groups consisting of 10 mice each, including the model group, the BZ-low group, the BZ-high group and the RAPA group. The BZ-low group and the BZ-high group were given 0.5 g/kg/d and 1 g/kg/d BZBS, respectively. The RAPA group was given 2 mg/kg/d rapamycin. Medicated feed was adopted as a drug delivery method. BZBS was provided by Hebei Shijiazhuang Yiling Pharmaceutical Co., Ltd. The study lasted for 6 months. The animal protocol was approved by the Ethics Commission of the Hebei Yiling Chinese Medicine Research Institute (N2021087).

2.2 Hematoxylin and eosin staining

The mice were anesthetized by pentobarbital sodium and sacrificed. Then ileum tissue samples from each mouse were separated. And the samples were fixed with 4% paraformaldehyde. Then they were cut into slices with a thickness of $5\ \mu\text{m}$, and stained with hematoxylin and eosin (H&E). Finally, the pathological change was observed under a light microscope (Leica Microsystems, Wetzlar, Germany). The length of intestinal villi was calculated by Image Pro Plus 6.0 software. The protocol was performed as previously described (Xu et al., 2023).

2.3 Nissl staining

According to the manufacturer's instructions, the Nissl staining kit (Beyotime, Shanghai, China) was used for staining (Ji et al., 2022). In brief, the sections were placed in toluidine blue at 60°C for 40 min. Then the sections were washed by distilled water. After being placed in 95% ethanol for rapid differentiation, the sections were transferred to anhydrous ethanol for rapid dehydration. Finally, the results were observed under a light microscope ($\times 400$ magnification).

2.4 Immunofluorescence staining

For immunofluorescence (IF), the ileum tissue samples were fixed in 4% paraformaldehyde, and then sectioned. The sections were repaired by microwave heating with 0.01 M sodium citrate antigen retrieval buffer. After incubated with hydrogen peroxide solution, the sections were sealed with 5% BSA at room temperature for 30 min. Then the sections were incubated with ZO-1 (Servicebio, GB111402, 1:500 dilution, China) and Occludin (Servicebio, GB111401, 1:500 dilution, China) overnight at 4°C . After being washed with PBS, the sections were incubated with Alexa Fluor 488 (Servicebio, GB25303, 1:500 dilution, China) and Coralite594 (Proteintech, SA00013-3-100,

1:300 dilution, China). Finally, images were captured with an inverted fluorescence microscope (Leica Microsystems, Wetzlar, Germany). Quantification of the positive area was performed using Image Pro Plus 6.0 software. The standard procedure was the same as that used in our previous study (Mao et al., 2023).

2.5 Immunohistochemistry staining

For immunohistochemistry (IHC), the sections were incubated with primary antibodies at 4°C overnight. Then, the reacted sections were incubated with the corresponding secondary antibody. After that, the sections were treated with the newly prepared DAB solution. Here, primary antibodies against F4/80 (Abcam, ab300421, 1:5000 dilution, United States), Ki67 (Abcam, ab15580, 1:1000 dilution, United States) and Lgr5 (Affinity, DF2816, 1:200 dilution, United States) were probed, respectively. Finally, the results were observed under a light microscope. All experiments followed the manufacturer's instructions (Yang X. et al., 2020; Yang H. H. et al., 2020).

2.6 Real-time quantitative PCR

Total RNA from the ileum tissues was extracted using the TransZol Up Plus RNA Kit (TransGen Biotech, ER501-01, China) followed by cDNA synthesis using the GoScript™ Reverse Transcription System (Promega, A5001, United States). Then, the quantitative real-time PCR was performed using the MonAmp™ ChemoHS qPCR Mix kit (Monad, MQ00401S, China). All experiments followed the manufacturer's instructions. The primers were shown in the Table 1. The standard procedure was the same as that used in our previous study (Ji et al., 2022).

2.7 Western blotting assay

The total protein of ileum tissues for western blotting was extracted, and the protein concentration was determined by a BCA protein assay kit following the manufacturer's instructions. Then the protein was separated by SDS-PAGE. After being separated, the protein was transferred onto PVDF membrane. Subsequently, the membrane was blocked with 5% BSA, and incubated with primary antibodies. Here, Cleaved caspase-1 (Affinity, AF4005, United States), NLRP3 (Servicebio, GB114320, China), Cleaved GSDMD (Abcam, ab255603, United States) and GAPDH (Servicebio, GB11002, China) antibodies were used and blots were quantified using ImageJ Software (NIH, Bethesda, MD, United States). Each group was tested using three samples. The results were normalized to the GAPDH band. The standard procedure was the same as that used in our previous study (Yang X. et al., 2020; Yang H. H. et al., 2020).

2.8 Enzyme-linked immunosorbent assay (ELISA)

According to the manufacturer's instructions, the expression level of LPS in the liver was measured using the ELISA kit (Cusabio,

TABLE 1 Sequences of primers used for qRT-PCR in this study.

Primer	Forward	Reverse
P53	CCCCTGTCATCTTTTGTCCCT	AGCTGGCAGAATAGCTTATTGAG
TNF- α	AGTGACAAGCCTGTAGCCC	GAGGTTGACTTTCTCCTGGTAT
NF- κ B	GACACGAACAGAATCCTCAGCATCC	CCACCAGCAGCAGCAGACATG
IL-4	GGTCTCAACCCCGAGTAGT	GCCGATGATCTCTCTCAAGTGAT
IL-6	TGTATGAACAACGATGATGCACTT	ACTCTGGCTTTGTCTTTCTTGTATCT
IL-10	CCTCGTTTGTACCTCTCTCCG	AGGACACCATAGCAAAGGGC
IL-1 β	CAGGATGAGGACATGAGCACC	CTCTGCAGACTCAAACCTCCAC
IL-18	AGCTTGTGAAAAAGAGAGAGACCT	GCTAGTCTTCGTTTGAACAGTGA
GAPDH	TGGATTGGACGCATTGGTC	TTTGCACTGGTACGTGTTGAT

CSB-E13066m, China). First, the standards and the samples were added to the reaction wells (100 μ L/well), and then, a negative control was set up, incubated for 1.5 h. To each well, horseradish peroxidase (HRP)-labeled streptavidin (100 μ L/well) was added, followed by 30 min of incubation. Then, the plate was incubated for 30 min in the dark with the chromogenic solution. After that, the termination solution was added to terminate the reaction. Eventually, the OD values of the wells were evaluated using a microplate reader (Beckman, Germany) at 450 nm.

2.9 *In vivo* two-photon imaging assay

To assay the permeability of the blood–brain barrier (BBB), the mice were anesthetized and placed on a head-fixing apparatus under a custom-modified two-photon microscope (Scientifica, Uckfield, United Kingdom). A dye mixture containing 12.5 mg/mL fluorescein isothiocyanate (FITC)-conjugated dextran (70 kDa molecular weight, Sigma-Aldrich, US) and 6.25 mg/mL tetramethylrhodamine (TRITC)-conjugated dextran (40 kDa molecular weight, Thermo Fisher Scientific, United States) was administered via tail vein injection. *In vivo* image stacks were then acquired. The protocol was performed as previously described (Lee et al., 2018).

2.10 16S rRNA gene sequencing

Fresh fecal samples of the three groups (the control group, the model group and the BZ-high group) were collected for 16S rRNA gene sequencing ($n = 10$). The procedure was performed as previously described (Bolyen et al., 2019).

2.11 Statistical analysis

The data were expressed as mean \pm SD, and all statistical analyses and graphing were performed using SPSS 26.0 (SPSS, Armonk, United States) and GraphPad Prism 8.0.2 (GraphPad, San Diego, United States). Differences among groups were determined using the one-way analysis of variance (ANOVA), and Tukey's test was used for *post hoc* comparisons. $p < 0.05$ was considered as a significant difference.

3 Results

3.1 BZBS improved the cognitive function in SAMP8 mice

To measure the number of neurons, Nissl staining was used in our study. The results showed that the number of neurons in the cortex and hippocampus of the model group was significantly decreased compared with that in the control group. Furthermore, BZBS treatment increased the neuronal numbers in the SAMP8 mice (Figures 1A,B). To assay the integrity of the BBB in the SAMP8 mice, we performed *in vivo* two-photon imaging to detect extravasation in the cerebral cortex. We observed extravasation of 40 kDa TRITC-conjugated dextran in the model group, signifying increased BBB leakage. Consistent with our hypothesis, BZBS treatment reduced the extravasation in the cerebral cortex (Figure 1C). These results fully reflected the protective effect of BZBS on the cognitive function in the SAMP8 mice.

3.2 BZBS ameliorated the intestinal barrier function in SAMP8 mice

In our study, the morphological change was assessed by H&E and IF staining. The results of H&E staining showed that the intestinal barrier of SAMP8 mice was damaged with reduced amounts of intestinal villi in the model group when compared with this in the control group. And BZBS treatment could reduce damage to intestinal barrier function and repair intestinal villus structure (Figure 2A). Consequently, the increased protein expression of ZO-1 and occludin in ileum tissues of BZBS-treated mice were further confirmed by IF imaging, respectively, (Figures 2B,C).

3.3 BZBS inhibited the secretion of SASP factors and macrophage infiltration in SAMP8 mice

In this study, the gene expression level of SASP markers, including P53, TNF- α , NF- κ B and IL-6, all increased in the model group compared with the control group. In addition, the gene expression level of IL-4 and IL-10 decreased in the comparison between the

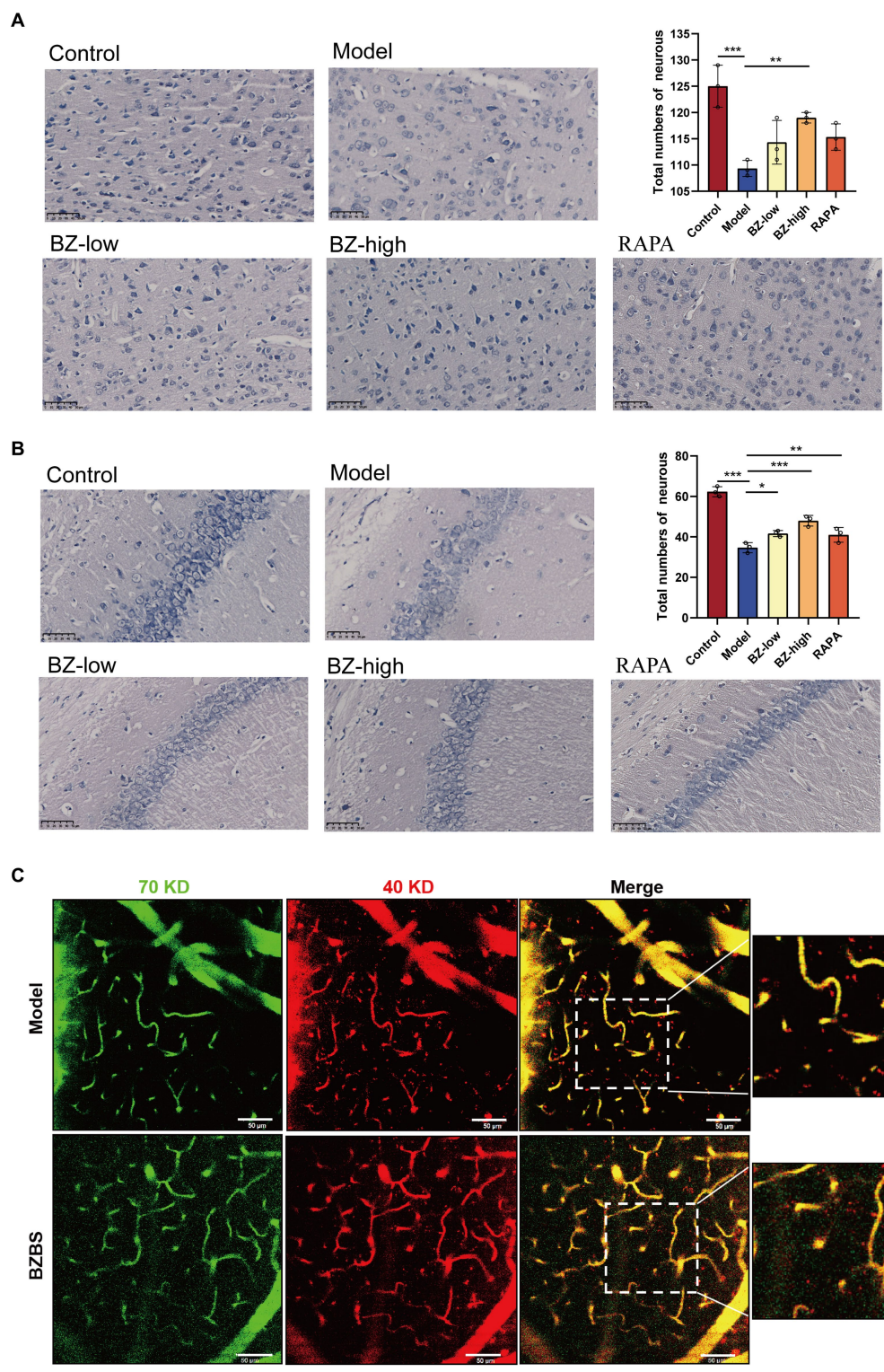


FIGURE 1
Effects of BZBS on the cognitive function in SAMP8 mice. **(A)** The result of Nissl staining in the cortex. **(B)** The result of Nissl staining in the hippocampus. **(C)** The result of *in vivo* two-photon imaging assay (* $p < 0.05$; ** $p < 0.01$; *** $p < 0.001$).

model group and the control group. Moreover, these parameters were normalized by BZBS administration. These results clearly demonstrated that BZBS administration inhibited the secretion of SASP factors in the SAMP8 mice (Figure 3A). In addition, the sections

were used to detect the expression level of F4/80 by IHC in the SAMP8 mice. The results indicated that F4/80 expression was increased in the model group. And these parameters were normalized by BZBS administration (Figure 3B).

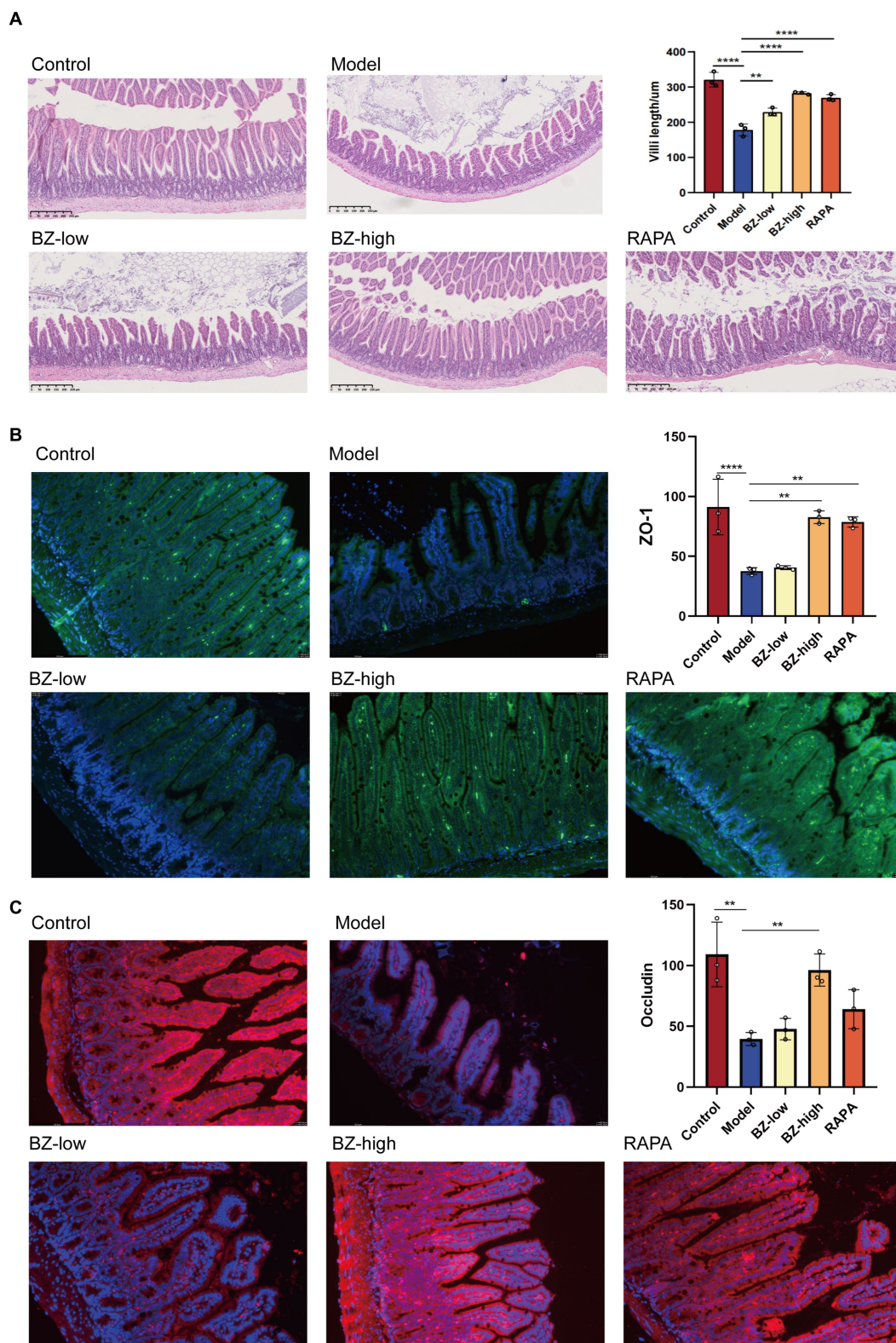


FIGURE 2
 Effects of BZBS on the intestinal barrier function in SAMP8 mice. **(A)** The result of H&E staining. **(B)** The result of ZO-1 expression level by immunofluorescence staining. **(C)** The result of occludin expression level by immunofluorescence staining (* $p < 0.05$; ** $p < 0.01$; *** $p < 0.001$; **** $p < 0.0001$).

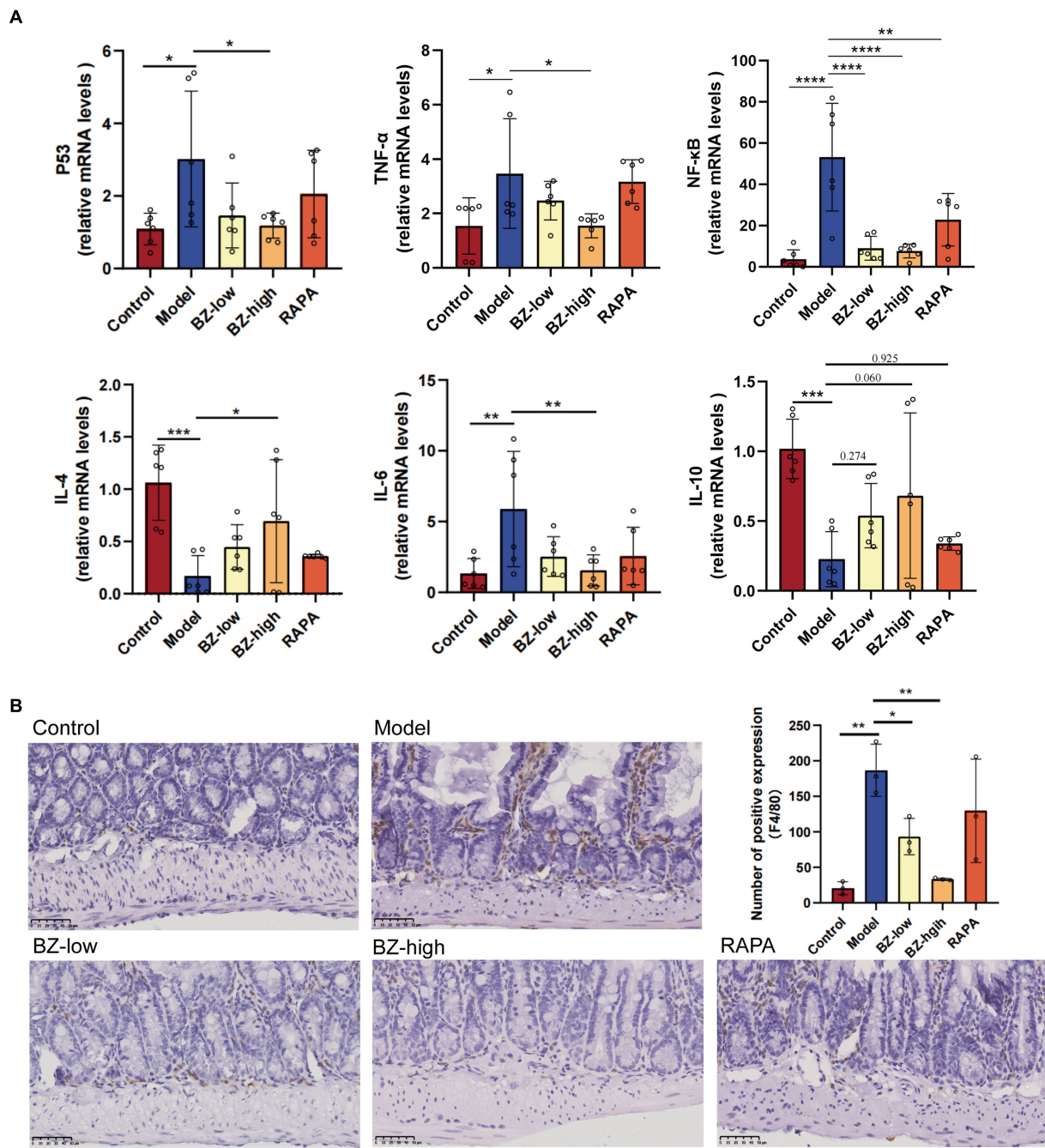


FIGURE 3 Effects of BZBS on the SASP in SAMP8 mice. **(A)** The result of mRNA expression level, including P53, TNF- α , NF- κ B, IL-4, IL-6, IL-10. **(B)** The result of F4/80-positive macrophages in ileum sections in the SAMP8 mice (* $p < 0.05$; ** $p < 0.01$; *** $p < 0.001$; **** $p < 0.0001$).

3.4 BZBS contributed to the regulation of intestinal cell proliferation and differentiation in SAMP8 mice

Intestine undergoes a continual process of proliferation and differentiation. In our study, we observed decreased proliferation of intestinal cell in the model group as noted by decreased expression of Ki67. Moreover, these parameters were normalized by BZBS administration (Figure 4A). As BZBS promoted crypt

cell proliferation, we postulated that BZBS might also play a role in regulating intestinal stem cell (ISC) activity. To investigate this hypothesis, we next determined the effect of BZBS on ISC marker. Compared with those in the control group, the levels of the ISC marker *Lgr5* were downregulated in the model group. Moreover, these parameters were normalized by BZBS administration (Figure 4B). These results indicated that BZBS may contribute to the processes of intestinal cell proliferation and differentiation.

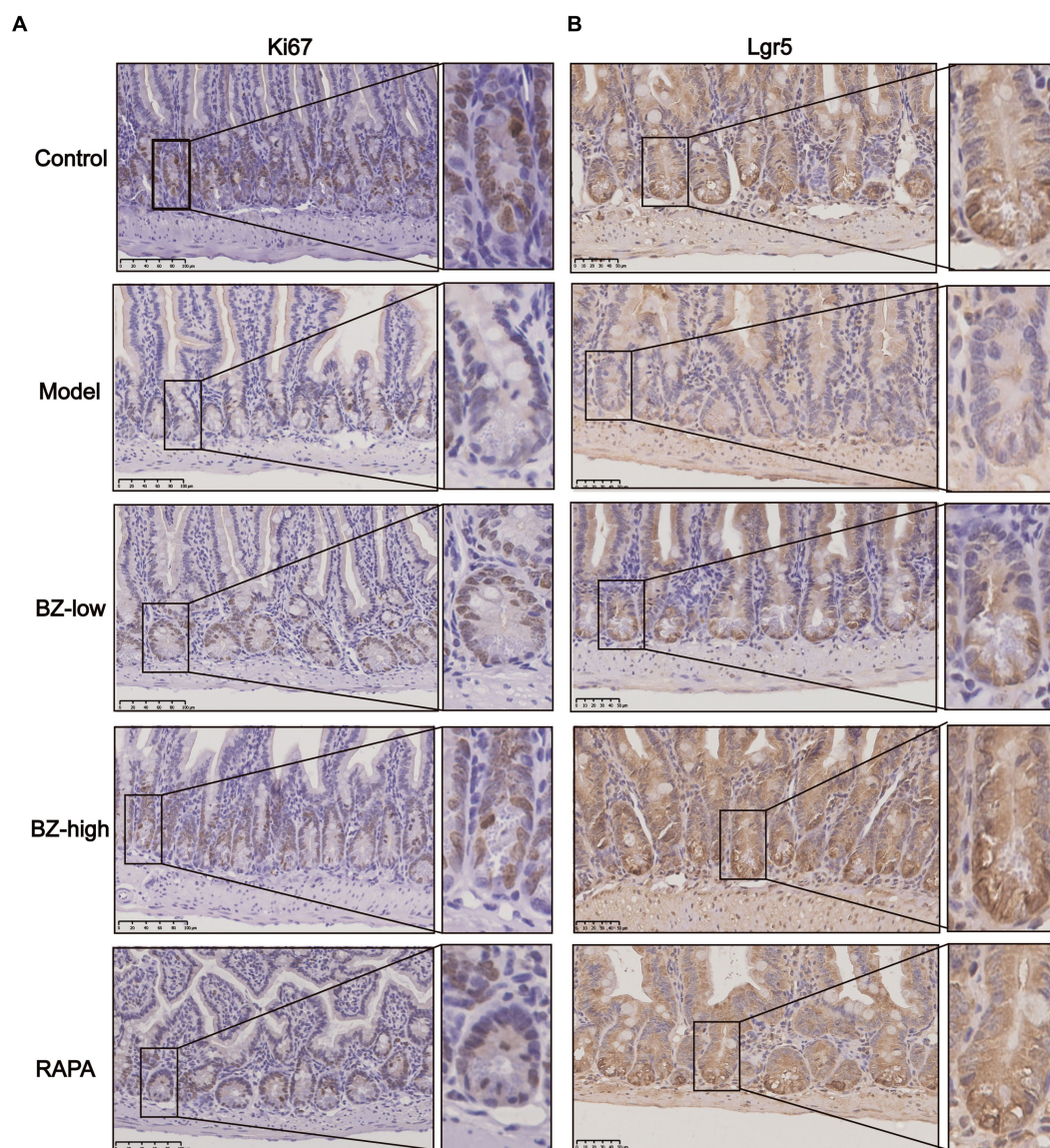


FIGURE 4
Effects of BZBS on regulation of proliferation and differentiation. **(A)** The result of proliferation level, and the molecular indicator of proliferation is Ki67. **(B)** The result of differentiation level, and the molecular indicator of proliferation is Lgr5.

3.5 BZBS treatment altered gut microbiota composition in SAMP8 mice

In this study, we analyzed the effect of BZBS on the gut microbiome by 16S rRNA gene sequencing. There was no significant difference between the model group and the BZ-high group in α -diversity (Figure 5A), whereas β -diversity analysis showed significant differences in the composition and abundance of the microbiome (Figure 5B). Linear discriminant analysis effect size (LEfSe) analysis revealed that the phylum *Bacteroidetes*, the families *Atopobiaceae*, *Bacteroidaceae*, *Mutibaculaceae* and *Prevotellaceae*, the genera *Atopobium*, *Bacteroides*, *Duncaniella*, *Muribaculum*, *Alloprevotella* and *Prevotella* were enriched in the model group, whereas the phylum *Firmicutes*, the families

Ruminococcaceae and *Lachnospiraceae*, the genera *Ruminococcaceae_UCG_014*, *Ruminococcaceae_UCG_004*, *Ruminiclostridium_9*, *Ruminiclostridium_5*, *Ruminiclostridium*, *Oscillibacter*, *Neglecta*, *Intestinimonas*, *Peptococcus*, *Roseburia*, *Eubacterium_xylanophilum_group*, *Anaerostignum*, *Acetatifactor* and *Eubacterium_brachy_group* were enriched in the BZ-high group (Figures 5C,D). The relative abundance of *Firmicutes/Bacteroidetes* ratio was significantly decreased in the model group, while the relative abundance was increased in the BZ-high group (Figure 5E). In detail, *Firmicutes* was the dominant bacteria in the BZ-high group, while *Bacteroidetes* was the dominant bacteria in the model group (Figure 5F). These results indicated that the BZ-high group had a unique intestinal microbiome composition compared with the model group.

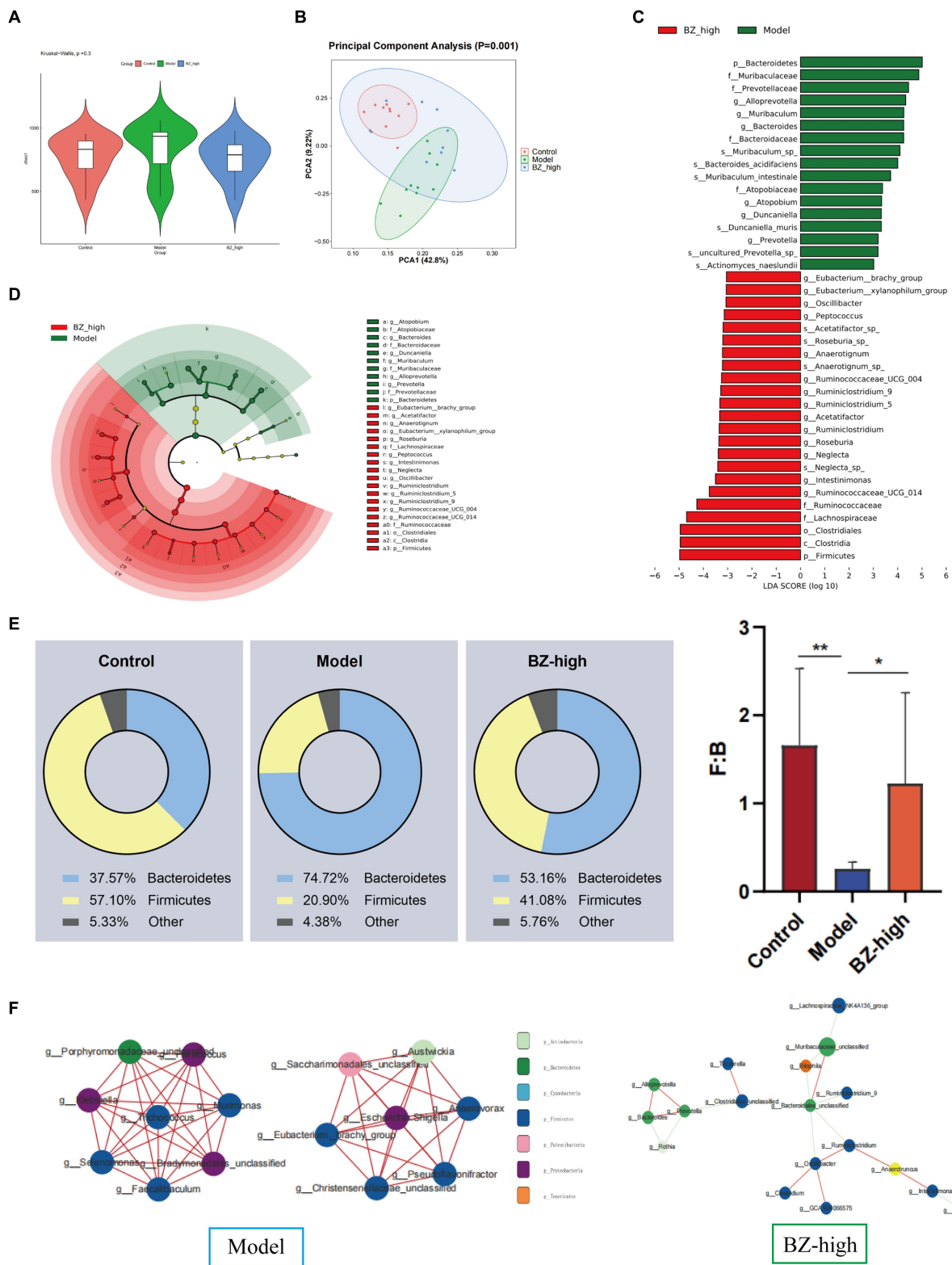


FIGURE 5 Effects of BZBS on the intestinal microbiota homeostasis in SAMB8 mice. **(A)** α diversity by Chao 1 index. **(B)** β diversity by PCA. **(C)** LDA score representing the taxonomic data with significant difference between the model group and the BZ-high group. **(D)** Taxonomic cladogram generated from LefSe analysis of 16s rRNA gene sequencing. **(E)** Results of comparison between Bacteroidetes and Firmicutes. **(F)** Results of dominant bacteria among different groups ($*p < 0.05$; $**p < 0.01$).

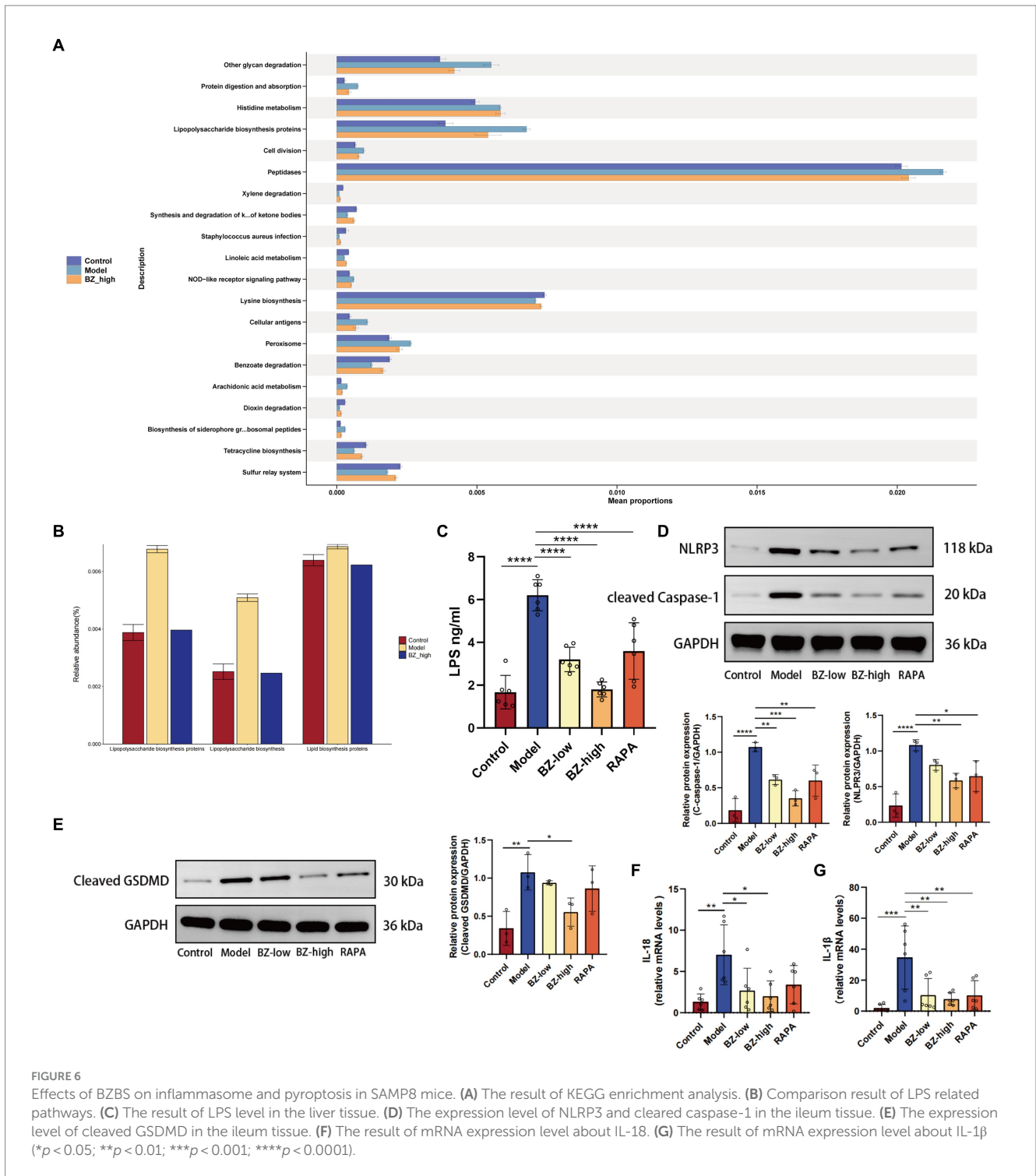


FIGURE 6 Effects of BZBS on inflammasome and pyroptosis in SAMP8 mice. **(A)** The result of KEGG enrichment analysis. **(B)** Comparison result of LPS related pathways. **(C)** The result of LPS level in the liver tissue. **(D)** The expression level of NLRP3 and cleared caspase-1 in the ileum tissue. **(E)** The expression level of cleaved GSDMD in the ileum tissue. **(F)** The result of mRNA expression level about IL-18. **(G)** The result of mRNA expression level about IL-1β (**p* < 0.05; ***p* < 0.01; ****p* < 0.001; *****p* < 0.0001).

3.6 BZBS inhibited inflammasome-mediated pyroptosis to reduce the intestinal damage in SAMP8 mice

To determine the mechanism of BZBS in prevention of intestinal barrier damage, the relative abundance of KEGG pathway was predicted by phylogenetic reconstruction of unobserved states 2 (PICRUST2) and the functional change of gut microbiota after BZBS

treatment was identified. The results revealed that lipopolysaccharide biosynthesis proteins were significantly enhanced in the model group (Figures 6A,B). To clarify the role of LPS in resulting in the intestinal damage, we tested the level of LPS in the liver by ELISA. The results indicated that LPS translocation due to intestinal barrier damage was reduced by BZBS (Figure 6C). Next, we measured the expression of NLRP3 and cleaved caspase-1, two markers of inflammasome activation, and the level of cleaved GSDMD, a marker of pyroptosis, in each group. As shown in the results, BZBS inhibited the expression

of NLRP3 and cleaved caspase-1, in a concentration-dependent manner as evidenced by western blot analysis (Figure 6D). In addition, the results also showed that BZBS could inhibit pyroptosis (Figure 6E). Moreover, the inhibitory effect of BZBS on the release of IL-1 β and IL-18 was further confirmed by real time PCR (Figures 6F,G).

4 Discussion

SAMP8 is a common model for studying accelerated aging (Morley et al., 2012; Cheng et al., 2014). In line with previous studies, we found that the SAMP8 mice had significantly fewer neurons, as shown by Nissl staining (Figures 1A,B) (Yang X. et al., 2020; Yang H. H. et al., 2020; Zhang N. et al., 2022; Zhang Y. et al., 2022). This result, together with the two-photon analysis, indicated that the SAMP8 mice show significant neuroinflammation and BBB disruption (Figure 1C). Moreover, we observed that the intestinal barrier function of the SAMP8 mice was impaired, as evidenced by the damage of the villous structure (Figure 2A). Our previous research has identified a wealth of bioactive compounds in BZBS that directly influence intestinal barrier function and the gut-brain axis (Huang et al., 2021). Chlorogenic acid, a prominent constituent, has been shown to enhance intestinal barrier integrity by alleviating endoplasmic reticulum stress and inhibiting ROCK/MLCK signaling pathways (Song et al., 2022). Additionally, flavonoids found in BZBS have been demonstrated to modulate the gut-brain axis, potentially improving age-related cognitive decline (Chu et al., 2023). These findings highlight the potential of BZBS to exert beneficial effects on intestinal health and cognitive function through its unique blend of bioactive compounds. In this experiment, we confirmed that BZBS treatment improved the integrity of the gut epithelial barrier by increasing the expression of tight junction proteins, and reduced neuroinflammation and enhanced cognitive function (Figures 2–4). Specifically, BZBS reshaped the gut microbiota community in SAMP8 mice, which in turn strengthened the intestinal integrity and suppressed inflammation (Figure 5). Mechanistically, we detected that BZBS treatment markedly prevented the cell pyroptosis by inhibiting the formation of inflammasome in the intestinal tissues of SAMP8 mice (Figure 6).

SAMP8 mice are a common model of accelerated aging that have cognitive and intestinal problems as they age (Yamamoto et al., 2015; Ben Othman et al., 2020; Chen et al., 2021). The gut-brain axis, which is the bidirectional communication between the gut and the brain (Xie et al., 2020; Chen et al., 2021; Zhang N. et al., 2022; Zhang Y. et al., 2022), may be involved in these problems (Xie et al., 2020; Yang X. et al., 2020; Yang H. H. et al., 2020; Yang D. et al., 2023; Yang X. Q. et al., 2023). Many studies have shown that gut dysbiosis, which is the imbalance of the gut microbiota, is associated with not only gastrointestinal diseases, but also the physiology and inflammation of the central nervous system (Ma et al., 2019; Rutsch et al., 2020; Morais et al., 2021). Some studies suggest that the gut dysbiosis may precede and affect the brain health in SAMP8 mice (Pellegrini et al., 2020; D'Antongiovanni et al., 2021). Similar gut-brain connections have been found in other models of Alzheimer's disease (AD), such as APP/PS1 and 5xFAD mice (Stoye et al., 2020; Guilherme et al., 2021), as well as in normal aging mice (Li T. et al., 2023). Therefore, the gut-brain axis may be a key factor for both cognitive function and

longevity (Dumic et al., 2019; Li et al., 2021; Hodge et al., 2022), and SAMP8 mice are a useful model to study how the gut-brain axis works and how drugs that target this axis can improve health and lifespan. We have previously shown that BZBS could effectively improve the cognitive aging caused by D-galactose exposed mice (Ji et al., 2022). Since the gut-brain axis plays an important role in central aging, we wanted to see if BZBS improves central aging through this axis.

Consistent with previous results, we found that SAMP8 mice not only showed increased BBB disruption with age, but also severe intestinal damage (Figures 1, 2). Here, we demonstrated that the SAMP8 mice, as an accelerated aging model, exhibit increased secretion of SASP accompanied by gut dysbiosis (Figure 3), which is consistent with previous studies that aging can lead to gut dysbiosis (Ling et al., 2022). Considering that gut dysbiosis causes central nervous inflammation through the gut-brain axis, we prioritized the detection of gut microbiota changes in the SAMP8 mice, finding a decrease in the ratio of Firmicutes to Bacteroides (F/B) with aging (Vaiserman et al., 2017). Compelling evidence shows that the ratio imbalance of F/B may activate inflammasome in the intestine by increasing the level of LPS, a bacterial toxin (Yu et al., 2017; Paik et al., 2021; Zhang N. et al., 2022; Zhang Y. et al., 2022). Furthermore, the activated inflammasome induces pyroptosis, a type of cell death that releases inflammatory cytokines, and causes intestinal injuries (Kovacs and Miao, 2017). The intestinal barrier damage would allow excessive LPS to enter the bloodstream, fallen into a vicious circle to accelerate systemic aging (Ising et al., 2019; Yang X. et al., 2020; Yang H. H. et al., 2020; de Carvalho Ribeiro and Szabo, 2022; Toldo et al., 2022). BZBS could reshape the decrease in the ratio of F/B and enhance intestinal integrity (Figure 5). Moreover, the KEGG pathways of gut microbiota revealed that LPS biosynthesis proteins was enhanced significantly in SAMP8 mice, and BZBS treatment restored the increased the LPS biosynthesis pathway (Figures 6A,B). LPS translocation owing to intestinal barrier damage was reduced by BZBS by detecting the level of LPS in the liver among groups (Figure 6C).

NLRP3 inflammasome activates pyroptosis, a type of cell death that releases inflammatory cytokines (Elliott and Sutterwala, 2015; Paik et al., 2021). When NLRP3 inflammasome is overactivated, it can cause chronic inflammation in the intestine and disrupt the balance of intestinal cell proliferation and differentiation (Lamkanfi et al., 2007). To further explore the underlying mechanism of BZBS in prevention of intestinal barrier damages, the biomarkers of inflammasome and pyroptosis were measured in each group. We found that BZBS modulated the gut microbiota and its metabolites, and inhibited NLRP3 inflammasome-mediated pyroptosis in the intestine of SAMP8 mice. We measured the expression of NLRP3 and cleaved caspase-1, two markers of inflammasome activation, and the levels of IL-1 β and IL-18, two cytokines released by pyroptosis, in each group. We showed that BZBS reduced the expression of NLRP3 and cleaved caspase-1, and the levels of IL-1 β and IL-18, in a dose-dependent manner (Figure 6). We also assessed the expression of Ki67 and Igr5, two indicators of intestinal stem cell activity, and found that BZBS enhanced the processes of intestinal cell proliferation and differentiation (Figure 3). Therefore, our study suggested that BZBS protected the intestine and cognition of SAMP8 mice by suppressing NLRP3 inflammasome-mediated pyroptosis via altering the gut microbiota and its metabolites.

This study explored the therapeutic potential of the compound TCM formula BZBS for age-related cognitive decline. By investigating its effects on the gut-brain axis, we demonstrated that BZBS significantly improved cognitive function and reduced central inflammation associated with accelerated aging. These findings suggest promising therapeutic potential for BZBS in managing age-related cognitive impairment and neuroinflammation. While this study provides valuable insights, it is important to acknowledge its limitations. Our focus on the overall effectiveness based on phenotypes limited the investigation of specific active components and their mechanisms of action. Additionally, a deeper exploration of the advantages of BZBS's multi-pathway and multi-target approach compared to single-target drugs is crucial to understand its full therapeutic potential. Further research is needed to elucidate the specific active components and their mechanisms of action within BZBS, conduct robust clinical trials to assess the safety and efficacy of BZBS in human populations, and compare the effectiveness of BZBS's multi-pathway and multi-target approach against single-target drugs for age-related cognitive decline.

5 Conclusion

Here, we present a study on the therapeutic effects of BZBS, a traditional Chinese medicine, in intestinal damage caused by accelerated aging. We found BZBS protected the deterioration of the intestinal barrier function by modulating the gut microbiota and its metabolites, and by inhibiting the NLRP3 inflammasome-mediated pyroptosis. These results suggest the therapeutic effect of BZBS on aging-related central diseases, at least partially, targets the gut-brain axis. Meanwhile, our results also confirm the advantages and applications of SAMP8 mice for studying aging-related central aging-related diseases and developing drugs targeting the microbiota-gut-brain axis.

Data availability statement

The raw sequence data reported in this study have been deposited in the Genome Sequence Archive (Genomics, Proteomics & Bioinformatics 2021) in National Genomics Data Center (Nucleic Acids Res 2022), China National Center for Bioinformation / Beijing Institute of Genomics, Chinese Academy of Sciences (GSA: CRA014256) [<https://ngdc.cnbc.ac.cn/gsa>].

Ethics statement

The animal study was approved by the ethics commission of the Hebei Yiling Chinese Medicine Research Institute. The study was conducted in accordance with the local legislation and institutional requirements.

References

- Barnett, K. C., Li, S., Liang, K., and Ting, J. P. (2023). A 360° view of the inflammasome: mechanisms of activation, cell death, and diseases. *Cells* 186, 2288–2312. doi: 10.1016/j.cell.2023.04.025
- Ben Othman, S., Ido, K., Masuda, R., Gotoh, S., Hosoda-Yabe, R., Kitaguchi, K., et al. (2020). Senescence-accelerated mouse prone 8 mice exhibit specific morphological

Author contributions

SZ: Data curation, Methodology, Writing – original draft. ML: Methodology, Software, Validation, Writing – original draft. LC: Data curation, Investigation, Writing – original draft. XM: Formal analysis, Project administration, Writing – original draft. YJ: Formal analysis, Project administration, Writing – original draft. XS: Formal analysis, Project administration, Writing – original draft. KN: Formal analysis, Project administration, Writing – original draft. XL: Data curation, Methodology, Writing – original draft. RZ: Formal analysis, Project administration, Writing – original draft. YS: Data curation, Methodology, Writing – original draft. KM: Funding acquisition, Investigation, Supervision, Validation, Writing – original draft. HL: Data curation, Methodology, Writing – original draft. CW: Supervision, Writing – original draft. YH: Conceptualization, Methodology, Writing – review and editing. YW: Conceptualization, Data curation, Funding acquisition, Investigation, Writing – review and editing.

Funding

The author(s) declare financial support was received for the research, authorship, and/or publication of this article. This work was supported by the Strategic Consulting Project of the Chinese Academy of Engineering: Strategic research on anti-aging effect of Traditional Chinese Medicine (grant no. 2022-XY-45), the Natural Science Foundation of Hebei Province in China (grant no. 2022106065), High-level S&T Innovation and Entrepreneurship Talent Project of Shijiazhuang, Hebei, China (grant no. 07202203) and S&T Program of Hebei (no. 22372502D) and (no. E2020100001). Scientific Research Plan Project of Hebei Administration of Traditional Chinese Medicine (no. 2023391). S&T Project of Shijiazhuang (no. 231790133A).

Conflict of interest

The authors declare that the research was conducted in the absence of any commercial or financial relationships that could be construed as a potential conflict of interest.

Publisher's note

All claims expressed in this article are solely those of the authors and do not necessarily represent those of their affiliated organizations, or those of the publisher, the editors and the reviewers. Any product that may be evaluated in this article, or claim that may be made by its manufacturer, is not guaranteed or endorsed by the publisher.

changes in the small intestine during senescence and after pectin supplemented diet. *Exp. Gerontol.* 142:111099. doi: 10.1016/j.exger.2020.111099

Bolyen, E., Rideout, J. R., Dillon, M. R., Bokulich, N. A., Abnet, C. C., Al-Ghalith, G. A., et al. (2019). Reproducible, interactive, scalable and extensible microbiome data science using QIIME 2. *Nat. Biotechnol.* 37, 852–857. doi: 10.1038/s41587-019-0209-9

- Branca, J. J. V., Gulisano, M., and Nicoletti, C. (2019). Intestinal epithelial barrier functions in ageing. *Ageing Res. Rev.* 54:100938. doi: 10.1016/j.arr.2019.100938
- Chen, L. H., Wang, M. F., Chang, C. C., Huang, S. Y., Pan, C. H., Yeh, Y. T., et al. (2021). *Lactobacillus paracasei* PS23 effectively modulates gut microbiota composition and improves gastrointestinal function in aged SAMP8 mice. *Nutrients* 13:1116. doi: 10.3390/nu13041116
- Cheng, X. R., Zhou, W. X., and Zhang, Y. X. (2014). The behavioral, pathological and therapeutic features of the senescence-accelerated mouse prone 8 strain as an Alzheimer's disease animal model. *Ageing Res. Rev.* 13, 13–37. doi: 10.1016/j.arr.2013.10.002
- Chu, Z., Han, S., Luo, Y., Zhou, Y., Zhu, L., and Luo, F. (2023). Targeting gut-brain axis by dietary flavonoids ameliorate aging-related cognition decline: evidences and mechanisms. *Crit. Rev. Food Sci. Nutr.* 1–22, 1–22. doi: 10.1080/10408398.2023.2222404
- Cristófol, R., Porquet, D., Corpas, R., Coto-Montes, A., Serret, J., Camins, A., et al. (2012). Neurons from senescence-accelerated SAMP8 mice are protected against frailty by the sirtuin 1 promoting agents melatonin and resveratrol. *J. Pineal Res.* 52, 271–281. doi: 10.1111/j.1600-079X.2011.00939.x
- D'Antongiovanni, V., Pellegrini, C., Antonoli, L., Benvenuti, L., Di Salvo, C., Flori, L., et al. (2021). Palmitoylethanolamide counteracts enteric inflammation and bowel motor dysfunctions in a mouse model of Alzheimer's disease. *Front. Pharmacol.* 12:748021. doi: 10.3389/fphar.2021.748021
- de Carvalho Ribeiro, M., and Szabo, G. (2022). Role of the Inflammasome in liver disease. *Annu. Rev. Pathol.* 17, 345–365. doi: 10.1146/annurev-pathmechdis-032521-102529
- Dumic, I., Nordin, T., Jecmenica, M., Stojkovic Lalošević, M., Milosavljević, T., and Milovanovic, T. (2019). Gastrointestinal tract disorders in older age. *Can. J. Gastroenterol. Hepatol.* 2019, 6757524–6757519. doi: 10.1155/2019/6757524
- El Maï, M., Bird, M., Allouche, A., Targen, S., Şeriföglü, N., Lopes-Bastos, B., et al. (2023). Gut-specific telomerase expression counteracts systemic aging in telomerase-deficient zebrafish. *Nat. Aging* 3, 567–584. doi: 10.1038/s43587-023-00401-5
- Elliott, E. I., and Sutterwala, F. S. (2015). Initiation and perpetuation of NLRP3 inflammasome activation and assembly. *Immunol. Rev.* 265, 35–52. doi: 10.1111/immr.12286
- Funk, M. C., Zhou, J., and Boutros, M. (2020). Ageing, metabolism and the intestine. *EMBO Rep.* 21:e50047. doi: 10.15252/embr.202050047
- Gao, Y., Li, B., Liu, H., Tian, Y., Gu, C., Du, X., et al. (2021). *Cistanche deserticola* polysaccharides alleviate cognitive decline in aging model mice by restoring the gut microbiota-brain axis. *Ageing* 13, 15320–15335. doi: 10.18632/aging.203090
- Gavrilov, L. A., and Gavrilova, N. S. (2017). Is aging a disease? *Biodemographers' point of view. Adv Gerontol.* 30, 841–842.
- Guilherme, M. D. S., Nguyen, V. T. T., Reinhardt, C., and Endres, K. (2021). Impact of gut microbiome manipulation in 5xFAD mice on Alzheimer's disease-like pathology. *Microorganisms* 9:815. doi: 10.3390/microorganisms9040815
- Hao, M., Ding, C., Peng, X., Chen, H., Dong, L., Zhang, Y., et al. (2022). Ginseng under forest exerts stronger anti-aging effects compared to garden ginseng probably via regulating PI3K/AKT/mTOR pathway, SIRT1/NF-κB pathway and intestinal flora. *Phytomedicine* 105:154365. doi: 10.1016/j.phymed.2022.154365
- Haran, J. P., and McCormick, B. A. (2021). Aging, frailty, and the microbiome-how Dysbiosis influences human aging and disease. *Gastroenterology* 160, 507–523. doi: 10.1053/j.gastro.2020.09.060
- Hodge, F., Bajuszova, V., and van Oosten-Hawle, P. (2022). The intestine as a lifespan- and Proteostasis-promoting signaling tissue. *Front. Aging* 3:897741. doi: 10.3389/fragi.2022.897741
- Huang, D., Wang, X., Zhu, Y., Gong, J., Liang, J., Song, Y., et al. (2021). Bazi Bushen capsule alleviates post-menopausal atherosclerosis via GPER1-dependent anti-inflammatory and anti-apoptotic effects. *Front. Pharmacol.* 12:774792. doi: 10.3389/fphar.2021.658998
- Ising, C., Venegas, C., Zhang, S., Scheiblich, H., Schmidt, S. V., Vieira-Saecker, A., et al. (2019). NLRP3 inflammasome activation drives tau pathology. *Nature* 575, 669–673. doi: 10.1038/s41586-019-1769-z
- Ji, C., Wei, C., Li, M., Shen, S., Zhang, S., Hou, Y., et al. (2022). Bazi Bushen capsule attenuates cognitive deficits by inhibiting microglia activation and cellular senescence. *Pharm. Biol.* 60, 2025–2039. doi: 10.1080/13880209.2022.2131839
- Kovacs, S. B., and Miao, E. A. (2017). Gasdermins: effectors of pyroptosis. *Trends Cell Biol.* 27, 673–684. doi: 10.1016/j.tcb.2017.05.005
- Lamkanfi, M., Festjens, N., Declercq, W., Vanden Berghe, T., and Vandenabeele, P. (2007). Caspases in cell survival, proliferation and differentiation. *Cell Death Differ.* 14, 44–55. doi: 10.1038/sj.cdd.4402047
- Lee, S., Kang, B. M., Kim, J. H., Min, J., Kim, H. S., Ryu, H., et al. (2018). Real-time in vivo two-photon imaging study reveals decreased cerebro-vascular volume and increased blood-brain barrier permeability in chronically stressed mice. *Sci. Rep.* 8:13064. doi: 10.1038/s41598-018-30875-y
- Li, Y., Guo, Y., Aoki, L., Ma, C., Xiong, Z., Yuan, D., et al. (2023). Changes of colon in rats with different ages in response to lipopolysaccharide. *Curr. Med. Chem.* 30, 4492–4503. doi: 10.2174/0929867330666230113112803
- Li, H., Ni, J., and Qing, H. (2021). Gut microbiota: critical controller and intervention target in brain aging and cognitive impairment. *Front. Aging Neurosci.* 13:671142. doi: 10.3389/fnagi.2021.671142
- Li, T., Yang, S., Liu, X., Li, Y., Gu, Z., and Jiang, Z. (2023). Dietary neoagartetraose extends lifespan and impedes brain aging in mice via regulation of microbiota-gut-brain axis. *J. Adv. Res.* 52, 119–134. doi: 10.1016/j.jare.2023.04.014
- Ling, Z., Liu, X., Cheng, Y., Yan, X., and Wu, S. (2022). Gut microbiota and aging. *Crit. Rev. Food Sci. Nutr.* 62, 3509–3534. doi: 10.1080/10408398.2020.1867054
- Ma, L., Ni, Y., Wang, Z., Tu, W., Ni, L., Zhuge, F., et al. (2020). Spermidine improves gut barrier integrity and gut microbiota function in diet-induced obese mice. *Gut Microbes* 12, 1832857–1832819. doi: 10.1080/19490976.2020.1832857
- Ma, Q., Xing, C., Long, W., Wang, H. Y., Liu, Q., and Wang, R. F. (2019). Impact of microbiota on central nervous system and neurological diseases: the gut-brain axis. *J. Neuroinflammation* 16:53. doi: 10.1186/s12974-019-1434-3
- Mao, X., Hou, Y., Fang, C., Ma, K., Zhang, S., Guo, Z., et al. (2023). Bazi Bushen mitigates epigenetic aging and extends healthspan in naturally aging mice. *Biomed. Pharmacother.* 160:114384. doi: 10.1016/j.biopha.2023.114384
- Marín-Aguilar, F., Lechuga-Vieco, A. V., Alcocer-Gómez, E., Castejón-Vega, B., Lucas, J., Garrido, C., et al. (2020). NLRP3 inflammasome suppression improves longevity and prevents cardiac aging in male mice. *Ageing Cell* 19:e13050. doi: 10.1111/acel.13050
- Morais, L. H., Schreiber, H. L. 4th, and Mazmanian, S. K. (2021). The gut microbiota-brain axis in behaviour and brain disorders. *Nat. Rev. Microbiol.* 19, 241–255. doi: 10.1038/s41579-020-00460-0
- Morley, J. E., Farr, S. A., Kumar, V. B., and Armbricht, H. J. (2012). The SAMP8 mouse: a model to develop therapeutic interventions for Alzheimer's disease. *Curr. Pharm. Des.* 18, 1123–1130. doi: 10.2174/138161212799315795
- Paik, S., Kim, J. K., Silwal, P., Sasakawa, C., and Jo, E. K. (2021). An update on the regulatory mechanisms of NLRP3 inflammasome activation. *Cell. Mol. Immunol.* 18, 1141–1160. doi: 10.1038/s41423-021-00670-3
- Pellegrini, C., Daniele, S., Antonoli, L., Benvenuti, L., D'Antongiovanni, V., Piccarducci, R., et al. (2020). Prodromal intestinal events in Alzheimer's disease (AD): colonic Dysmotility and inflammation are associated with enteric AD-related protein deposition. *Int. J. Mol. Sci.* 21:3523. doi: 10.3390/ijms21103523
- Roig-Soriano, J., Griñán-Ferré, C., Espinosa-Parrilla, J. F., Abraham, C. R., Bosch, A., Pallàs, M., et al. (2022). AAV-mediated expression of secreted and transmembrane αKlotho isoforms rescues relevant aging hallmarks in senescent SAMP8 mice. *Ageing Cell* 21:e13581. doi: 10.1111/acel.13581
- Rutsch, A., Kantsjö, J. B., and Ronchi, F. (2020). The gut-brain Axis: how microbiota and host Inflammasome influence brain physiology and pathology. *Front. Immunol.* 11:604179. doi: 10.3389/fimmu.2020.604179
- Salazar, A. M., Aparicio, R., Clark, R. I., Rera, M., and Walker, D. W. (2023). Intestinal barrier dysfunction: an evolutionarily conserved hallmark of aging. *Dis. Model. Mech.* 16:dmm049969. doi: 10.1242/dmm.049969
- Soenen, S., Rayner, C. K., Jones, K. L., and Horowitz, M. (2016). The ageing gastrointestinal tract. *Curr. Opin. Clin. Nutr. Metab. Care* 19, 12–18. doi: 10.1097/MCO.0000000000000238
- Song, L., Wu, T., Zhang, L., Wan, J., and Ruan, Z. (2022). Chlorogenic acid improves the intestinal barrier by relieving endoplasmic reticulum stress and inhibiting ROCK/MLCK signaling pathways. *Food Funct.* 13, 4562–4575. doi: 10.1039/d1fo02662c
- Stoye, N. M., Dos Santos Guilherme, M., and Endres, K. (2020). Alzheimer's disease in the gut-major changes in the gut of 5xFAD model mice with Apo A1 as potential key player. *FASEB J.* 34, 11883–11899. doi: 10.1096/fj.201903128RR
- Sun, C., Chen, X., Yang, S., Jin, C., Ding, K., and Chen, C. (2023). LBP1C-2 from *Lycium barbarum* alleviated age-related bone loss by targeting BMPRIA/BMPRII/noggin. *Carbohydr. Polym.* 310:120725. doi: 10.1016/j.carbpol.2023.120725
- Suzuki, T., Aoki, K., Shimokobe, K., Omiya, S., Funayama, C., Takahashi, T., et al. (2022). Age-related morphological and functional changes in the small intestine of senescence-accelerated mouse. *Exp. Gerontol.* 163:111795. doi: 10.1016/j.exger.2022.111795
- Toldo, S., Mezzaroma, E., Buckley, L. F., Potere, N., Di Nisio, M., Biondi-Zoccai, G., et al. (2022). Targeting the NLRP3 inflammasome in cardiovascular diseases. *Pharmacol. Ther.* 236:108053. doi: 10.1016/j.pharmthera.2021.108053
- Vaiserman, A. M., Koliada, A. K., and Marotta, F. (2017). Gut microbiota: a player in aging and a target for anti-aging intervention. *Ageing Res. Rev.* 35, 36–45. doi: 10.1016/j.arr.2017.01.001
- Wang, D., Chang, L., Hao, J., Zhang, J., Song, Y., Ma, K., et al. (2023). Estrogen-like effect of Bazi Bushen capsule in ovariectomized rats. *J. Vis. Exp.* 194. doi: 10.3791/64884
- Xie, Z., Lu, H., Yang, S., Zeng, Y., Li, W., Wang, L., et al. (2020). Salidroside attenuates cognitive dysfunction in senescence-accelerated mouse prone 8 (SAMP8) mice and modulates inflammation of the gut-brain Axis. *Front. Pharmacol.* 11:568423. doi: 10.3389/fphar.2020.568423

- Xu, Z., Man, S. S., Gong, B. Y., Li, Z. D., Zhou, H. F., Peng, Y. F., et al. (2023). Bazi Bushen maintains intestinal homeostasis through inhibiting TLR4/NF κ B signaling pathway and regulating gut microbiota in SAMP6 mice. *J. Sci. Food Agric.* 103, 7273–7283. doi: 10.1002/jsfa.12812
- Yamamoto, K. E. S., Hatakeyama, Y., Sakamoto, Y., and Tsuduki, T. (2015). High-fat diet intake from senescence inhibits the attenuation of cell functions and the degeneration of villi with aging in the small intestine, and inhibits the attenuation of lipid absorption ability in SAMP8 mice. *J. Clin. Biochem. Nutr.* 57, 204–211. doi: 10.3164/jcbrn.15-60
- Yang, H. H., Duan, J. X., Liu, S. K., Xiong, J. B., Guan, X. X., Zhong, W. J., et al. (2020). A COX-2/sEH dual inhibitor PTUPB alleviates lipopolysaccharide-induced acute lung injury in mice by inhibiting NLRP3 inflammasome activation. *Theranostics.* 10, 4749–4761. doi: 10.7150/thno.43108
- Yang, D., Wang, Z., Chen, Y., Guo, Q., and Dong, Y. (2023). Interactions between gut microbes and NLRP3 inflammasome in the gut-brain axis. *Comput. Struct. Biotechnol. J.* 21, 2215–2227. doi: 10.1016/j.csbj.2023.03.017
- Yang, X., Yu, D., Xue, L., Li, H., and Du, J. (2020). Probiotics modulate the microbiota-gut-brain axis and improve memory deficits in aged SAMP8 mice. *Acta Pharm. Sin. B* 10, 475–487. doi: 10.1016/j.apsb.2019.07.001
- Yang, X. Q., Zhao, Y., Xue, L., Wang, H. S., Zeng, J., Du, J. R., et al. (2023). Probiotics improve cognitive impairment by decreasing Bacteria-related pattern recognition receptor-mediated inflammation in the gut-brain Axis of mice. *J. Integr. Neurosci.* 22:92. doi: 10.31083/jjin2204092
- Yu, X., Lan, P., Hou, X., Han, Q., Lu, N., Li, T., et al. (2017). HBV inhibits LPS-induced NLRP3 inflammasome activation and IL-1 β production via suppressing the NF- κ B pathway and ROS production. *J. Hepatol.* 66, 693–702. doi: 10.1016/j.jhep.2016.12.018
- Zhang, Y., Zhang, S., Li, B., Luo, Y., Gong, Y., Jin, X., et al. (2022). Gut microbiota dysbiosis promotes age-related atrial fibrillation by lipopolysaccharide and glucose-induced activation of NLRP3-inflammasome. *Cardiovasc. Res.* 118, 785–797. doi: 10.1093/cvr/cvab114
- Zhang, N., Zhang, Y., Wang, Z., Pan, F., Ren, R., Li, Z., et al. (2022). Regular fecal microbiota transplantation to senescence accelerated mouse-prone 8 (SAMP8) mice delayed the aging of locomotor and exploration ability by rejuvenating the gut microbiota. *Front. Aging Neurosci.* 14:991157. doi: 10.3389/fnagi.2022.991157
- Zhao, C., Hu, X., Qiu, M., Bao, L., Wu, K., Meng, X., et al. (2023). Sialic acid exacerbates gut dysbiosis-associated mastitis through the microbiota-gut-mammary axis by fueling gut microbiota disruption. *Microbiome.* 11:78. doi: 10.1186/s40168-023-01528-8
- Zheng, M., and Kanneganti, T. D. (2020). The regulation of the ZBP1-NLRP3 inflammasome and its implications in pyroptosis, apoptosis, and necroptosis (PANoptosis). *Immunol. Rev.* 297, 26–38. doi: 10.1111/imr.12909